

## Full Length Article

## The effect of electron-surface scattering and thiol adsorption on the electrical resistivity of gold ultrathin films



Ricardo Henriquez <sup>a,\*</sup>, Valeria Del Campo <sup>a</sup>, Claudio Gonzalez-Fuentes <sup>a</sup>, Jonathan Correa-Puerta <sup>b</sup>, Luis Moraga <sup>c</sup>, Marcos Flores <sup>d</sup>, Rodrigo Segura <sup>e</sup>, Sebastián Donoso <sup>a</sup>, Francisca Marín <sup>a</sup>, Sergio Bravo <sup>a</sup>, Patricio Häberle <sup>a</sup>

<sup>a</sup> Departamento de Física, Universidad Técnica Federico Santa María, Av. España 1680, Valparaíso 2390123, Chile

<sup>b</sup> Instituto de Física, Pontificia Universidad Católica de Valparaíso, Av. Universidad 330, Curauma, Valparaíso, Chile

<sup>c</sup> Universidad Central de Chile, Toesca 1783, Santiago 8370178, Chile

<sup>d</sup> Departamento de Física, Facultad de Ciencias Físicas y Matemáticas, Universidad de Chile, Av. Blanco Encalada 2008, Santiago, Chile

<sup>e</sup> Instituto de Química y Bioquímica, Facultad de Ciencias, Universidad de Valparaíso, Av. Gran Bretaña 1111, Valparaíso, Chile

## ARTICLE INFO

## Article history:

Received 2 September 2016

Received in revised form 27 January 2017

Accepted 18 February 2017

Available online 24 February 2017

## Keywords:

Ultrathin films

Resistivity

Thiol

Electrical transport

Gold

## ABSTRACT

In order to study the effect of electron-surface scattering in gold ultrathin films ( $\sim 10$  nm), we have prepared a set of Au samples on mica on top of a chromium seedlayer ( $<1$  nm). Chromium is added as a metallic surfactant which enables surpassing the electric percolation threshold for substrate temperatures above room temperature. We prepared samples with the same thickness but different topographies setting different substrate temperatures. These modifications modulate the contributions of the different electronic scattering mechanisms to the film resistivity. A second set of gold thin films deposited on mica at room temperature, with different thicknesses between 8 and 100 nm, was also prepared to compare the resistivities of both sets through Mayadas and Shatzkes theory. We found that in samples with thicknesses below 15 nm, the electron-surface scattering is indeed the dominant mechanism influencing the film resistivity. To obtain further evidence of this prevalence, we developed a discrimination method based on thiol adsorption. The film with the highest resistivity increase is the sample in which electron-surface scattering is dominant. With this method, we observed that a large enhancement of the electron-surface scattering not only occurs in samples with large diameters grains, but also if the film has a reduced surface roughness.

© 2017 Elsevier B.V. All rights reserved.

## 1. Introduction

The miniaturization of the electronic circuits in current technology has called again into prominence the old problem of how the physical properties of an object are affected when one of its dimensions reaches the nanometric scale; or briefly, how their physical properties are affected by size effects. It is known that current devices, which function by means of electronic transport, have reached characteristic lengths of a few tens of nanometers [1]. Therefore, the investigation of the electrical properties of metallic films has to be extended from the thin to the ultrathin regime. That is, we must consider films with thicknesses comparable to a

small number of atomic diameters. The initial stages of film fabrication (for instance, from vacuum deposition onto a solid substrate) do not necessarily occur through the growth of a uniform thickness film capable of providing unambiguous paths for electronic transport. On the contrary, even if it is possible to establish a current through the sample, the transport may be more akin to the flow of a liquid through a porous medium, that is, rather a percolative than a conductive process. The crossing from the former to the latter behavior implies the formation of long range reconnections inside the material; which happens at the so called *percolation threshold*. If for very thin films, this percolation limit is not reached, hence a non-metallic electrical behavior is expected. The films are then characterized by a high resistance and a negative temperature coefficient [2].

One of the fundamental questions about electric transport in metallic films is to determine how each of the different microscopic scattering mechanisms, is affected by a reduction of the sample

\* Corresponding author.

E-mail addresses: [ricardo.henriquez@usm.cl](mailto:ricardo.henriquez@usm.cl), [\(R. Henriquez\).](mailto:rahc.78@gmail.com)

dimensions down to nanometric scales [3–5]. The resistivity of a metallic ultrathin film at room temperature may be understood as the result of three main electronic mechanisms: electron-phonon scattering, electron-surface scattering and electron-grain boundary scattering. These mechanisms can be related to characteristic lengths of the sample: bulk mean free path at room temperature, sample thickness and mean grain diameter, respectively. In order to understand how these processes combine in practice, we can engineer the fabrication procedures so that one of these mechanisms predominates over the others. Thus, to investigate the effect of electron-surface scattering, in 1964 Lucas [6] evaporated gold ultrathin films onto bismuth oxide substrates; and subsequently annealed them at 350 °C. Gold atoms were then deposited on the film surface at room temperature, and a resistivity increase was observed. This effect was attributed to a modification of the electron-surface scattering produced by the added Au atoms. These adatoms changed the film morphology from a flat to a rough surface. Another experiment, designed to clarify the nature of electron-surface scattering, was reported by H. Marom and M. Eizenberg [7] in 2006. They fabricated copper films with thicknesses between 50 and 90 nm. By annealing their samples at 300 °C, they diminished the surface roughness and obtained films in which the electron-grain boundary scattering was the dominant cause of the resistivity. Then, by an etching process in solution, they artificially created a surface roughness on these samples and observed a substantial rise in resistivity, clearly attributable to an increase in electron-surface scattering.

Whereas the main idea of these works was to understand the nature of electron-surface scattering through surface roughness modification, Henriquez et al. [8] investigated the combined influence of grain-boundary and surface scattering on the conductivity problem. They controlled the mean grain diameter by varying the substrate temperature, and identified the contribution of electron-surface scattering through measurements of the Hall mobility. They concluded that an enlargement of the mean grain diameter reduces the electron-grain boundary scattering, with a corresponding enhancement of the electron-surface scattering. Hence, the effect of the latter could be disentangled through film's surface modification. An alternative way to change the relative relevance of each process consists in the addition of scattering centers over the sample surface. This can be achieved by the formation of self-assembled monolayers (SAMs); which are ordered molecular overlayers that grow on the film [9]. One of the simplest ways to build these SAMs is through thiol adsorption from solution onto a metallic substrate [10]. Most thiols are bound to the surface by means of their S-head group, creating scattering centers and thus increasing the resistivity [9,11–13].

In this work, we present a fabrication procedure for gold ultrathin films on mica that maximizes the contribution of electron-surface scattering to the electrical resistance. Further, the identification of this scattering mechanism was made through an improved experimental method, based on the determination of the resistivity increase induced by thiol adsorption.

## 2. Theory

A widely used theory to describe the effect of electron-surface and electron-grain boundary scattering on the resistivity of thin films is the one published by Mayadas and Shatzkes (MS) in 1970 [14]. In this theory, the motion of the electrons is described by means of the Boltzmann transport equation and the contribution of grain boundaries is modeled by a series of Dirac  $\delta$  function potentials, distributed perpendicularly to the direction of the current, and characterized by a reflectivity coefficient  $R$ . This coefficient represents the fraction of electrons specularly reflected at the grain

boundary. The separation between adjacent delta potentials is a random variable, distributed according to a Gaussian function, with a mean distance  $D$  and a standard deviation  $s$ . We shall subsequently identify  $D$  as the mean grain diameter. The effect of electron-surface scattering is accounted by imposing a boundary condition over the electron distribution function, represented by a specularity parameter  $P$ . This coefficient is the same used in the Fuchs-Sondheimer theory [15,16] and denotes the fraction of carriers scattered by the surface at each interaction that remains in the out-of-equilibrium distribution, in turn the  $1-P$  fraction is scattered diffusely and increases the resistivity. This boundary condition was generalized by Lucas [17] who introduced two different specularity parameters  $P$  and  $Q$ , respectively associated to the upper and lower interface of the sample. Thus, the theoretical prediction for the quotient between film and bulk resistivity,  $(\rho/\rho_0)_{MS}$ , has seven input parameters:  $D$ ,  $s$ ,  $R$ ,  $P$ ,  $Q$ , film thickness  $t$  and bulk mean free path  $\lambda_0$ . The final expression used for calculating the resistivity is the one indicated in Reference [3].

The procedure we use to analyze the data with MS theory starts with the determination of the mean grain diameter  $D$  and its standard deviation  $s$  by means of scanning tunneling microscopy (STM). Also, the sample thickness  $t$  and the sample resistivity  $\rho$  are directly measured, while the values of the bulk resistivity  $\rho_0$  and bulk mean free path  $\lambda_0$  as a function of temperature are obtained from Reference [18]. Then, the values of  $R$ ,  $P$  and  $Q$  are determined through the best fit of the theory to the experimental data [19,20].

## 3. Materials and methods

To fabricate ultrathin films with metallic properties, we must first assert that the films have surpassed the electrical percolation threshold. The threshold thickness of the film, at which metallic behavior is obtained, depends on the particular film-substrate system [21] and on fabrication conditions, such as substrate temperature, annealing temperature [22] and deposition rate [8]. In order to study electrical properties of thin metallic films, gold has been widely used, mainly due the simplicity of its deposition and the absence of oxidation in atmospheric conditions. Furthermore, the preferred substrate for gold deposition is mica, due to the presence of atomically flat terraces that are easily obtained by cleavage [23].

At room temperature, the mean free path of gold is of the order of 40 nm. Therefore, in order to reveal the effect of electron-surface scattering at this temperature, it is necessary to fabricate samples with thicknesses at least comparable to this dimension. Furthermore, in order to reduce the effect of electron-grain boundary scattering, a clear experimental path is to fabricate samples with mean grain diameter larger than its thickness. A method to increase diameter is to deposit the films at a high temperature; or to anneal them after deposition. However, this process increases the thickness at which the percolation threshold is obtained. Kastle et al. [24] solved this problem by depositing, prior to fabrication, a metallic surfactant sandwiched between the substrate and the film. In this work, we used chromium as surfactant.

Samples preparation was performed through thermal evaporation from a tungsten basket in a High Vacuum System (base pressure  $\sim 3 \times 10^{-5}$  Pa), in which two or more materials could be evaporated sequentially. Evaporation rate and film thicknesses of gold (99.999% purity) and chromium (99.99% purity) were measured with quartz microbalances. These were previously calibrated by growing samples whose thicknesses were measured by ellipsometry and atomic force microscopy. The sample holder was made of copper with an oven in which a thermocouple was used to control deposition and annealing temperatures. A mask placed on the

substrate was used to generate samples with a four-contact geometry.

The mica surface and the chromium surfactant film were characterized by non-contact atomic force microscopy (NC AFM). The morphology of the gold films was characterized by scanning tunneling microscopy (STM). Two characteristic values were obtained from gold topographic images: mean grain diameter and the amplitude of the surface roughness. In order to measure the mean grain diameter, a series of topography images were recorded from different places on each sample. We identified grain boundaries and measured the enclosed areas. Then, we calculated the diameter of a circle that enclosed the same area. The histogram, generated with at least 500 diameters, shows a lognormal distribution, and its average is reported as the mean grain diameter  $D$ . To determine the amplitude of the surface roughness from the topographic images, we selected square shaped areas with different edge lengths and computed the standard deviation from the mean height in each square. These averaged roughness amplitudes, when plotted as a function of the edge length, reaches a saturation value for long edge lengths. In this work, we considered this value as the amplitude of the surface roughness.

The electrical characterization of ultrathin films was performed through the determination of resistivity at room temperature (RT). The four-contacts method was used to measure film resistance, injecting a current of  $15 \mu\text{A}$  with a frequency of  $540 \text{ Hz}$ . The measured voltage signals were acquired using a computer controlled 830's LIA built by Stanford Research.

Details about fabrication and characterization of the SAMs can be found in Reference [12]. Briefly, SAMs were prepared by immersing ultra thin films into a freshly prepared  $1 \text{ mM}$  solution of dodecanethiol ( $\text{C}_{12}\text{H}_{25}\text{SH}$ , 98% purity, Aldrich) in absolute ethanol (p.a. grade, Aldrich). The electrical resistance was monitored during thiols adsorption process. After 40 min, the SAM acquires full coverage with its characteristic ordered structure [9]. At this point, the resistivity increase due to the creation of the new scattering centers is essentially completed [9]. The increment in resistivity was determined comparing resistances measured before and after the sample was immersed inside the solution for 25 min. X-ray photoelectron spectroscopy (XPS) was used to verify the existence of the S-Au bond characteristic of the formation of a SAM on Au.

#### 4. Results and discussion

In order to grow films with large grains, we prepared gold ultra thin films (10 nm thick) onto mica with a chromium seed layer of 0.8 nm (Au/Cr/Mica). The difference among the films is the substrate temperature during growth,  $T_s$ , which varied between 320 K and 630 K. The electrical characterization was performed by measuring samples resistivity at room temperature (RT):  $\rho(\text{RT})$ .

For  $T_s \leq 390 \text{ K}$ , the measured resistivities turned out to be similar to the bulk value of Au ( $\sim 22 \text{ n}\Omega\text{m}$ ). However, for  $T_s \geq 460 \text{ K}$  we observed an increase in resistivity of at least three orders of magnitude. Further, these values for resistivity did not correlate with  $T_s$ . This behavior can be understood by noting that the thickness for percolation increases as the substrate temperature rises [22]. As expected, some of these films are far from being metallic. In order to obtain lower resistivities, we increased the thicknesses of these samples. This goal was achieved in an 18 nm thick sample, evaporated at 540 K.

Samples with  $\rho(\text{RT}) < 5000 \text{ n}\Omega\text{m}$  appear in Fig. 1 represented with stars markers. Numbers next to the symbols indicate substrate temperatures during deposition. Henceforth, only Au/Cr/Mica samples presenting values comparable with the corresponding bulk resistivity will be considered in the analysis below.

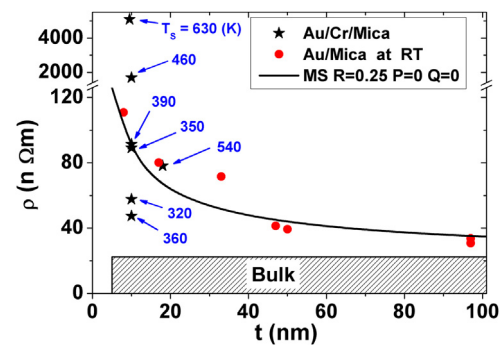


**Fig. 1.** Thickness dependence of the RT resistivity of a series of Au/Cr/Mica (star symbols) and Au/Mica (red circles) films. Au/Cr/Mica samples were evaporated at different substrate temperatures  $T_s$  indicated with numbers next to the markers. Au/Mica samples were deposited at room temperature. The continuous line is the best adjustment of MS theory for Au/Mica films. The hatched area represents the bulk resistivity.

A second series of gold films, with different thicknesses, were deposited on bare mica (Au/Mica) at room temperature. Morphological characterization of some samples is reported in Refs. [8,20,23]. Room temperature resistivity measurements of all samples are shown in Fig. 1.

In order to obtain a quantitative understanding of the scattering mechanism that contributes to the resistivity of our films, we analyzed the resistivity data of Au/Mica samples using the MS theory. In this analysis, we uniformly assumed  $\rho_0 = 22.4 \text{ n}\Omega\text{m}$  and  $\lambda_0 = 38 \text{ nm}$  [18]. Fig. 2a shows the evolution of the mean grain diameter, as a function of thickness for the Au/Mica samples. To apply this model, the thickness dependence of mean grain diameter  $D$  was obtained from a linear fit of the experimental data:  $D(t) = (0.3t + 10.1) \text{ nm}$ . With  $\rho_0$ ,  $\lambda_0$ , and  $D(t)$  as input data, we used the MS model to adjust the thickness dependence of the resistivity, and found that  $(R, P, Q) = (0.25, 0.0, 0.0)$ . Fig. 1, shows the resulting MS theoretical prediction as a solid black line.

Through this adjustment, a first comparison between the contributions of the different mechanisms to resistivity can be made [20]. For this purpose, we evaluated the output of the MS prediction by suppressing the effect of one mechanism at a time. That is, we calculated the resistivity predicted by MS without the effect of electron-grain boundary scattering, by setting  $R=0$ , and keeping the experimental values of  $P=Q=0.0$ . Subsequently, we compared the contribution of the surface roughness scattering with the values provided by the MS theory when the effect of electron-surface scattering is suppressed (only the grain-boundary scattering was considered) by setting  $P=Q=1.0$ , and preserving the true value of the grain boundary reflectivity  $R=0.25$ . A slight increase of the electron-grain boundary contribution was obtained as thickness decreases, but with values always comparable to the electron-phonon contribution ( $\sim 23 \text{ n}\Omega\text{m}$ ). On the other hand, the electron-surface contribution is small; increasing slightly as the thickness decreases down to  $\sim 25 \text{ nm}$ . From this thickness, the electron-surface contribution is significantly enhanced, until it exceeds the other scattering mechanisms below  $\sim 15 \text{ nm}$ . Since all Au/Cr/Mica samples present resistivities comparable to the Au/Mica resistivities (or smaller), we can conclude that, in the range  $t < 20 \text{ nm}$ , the contribution to the resistivity from the electron-surface scattering is relevant.

As previously discussed, the morphological characterization of the Au/Cr/Mica films was performed through the determination of mean grain diameter ( $D$ ) and surface roughness ( $\sigma$ ). Table 1 shows  $D$  and  $\sigma$  for each sample. Fig. 2a displays a comparison of the thickness dependence of  $D$  for Au/Cr/Mica and Au/mica samples. A significant increase of mean grain diameter is observed as

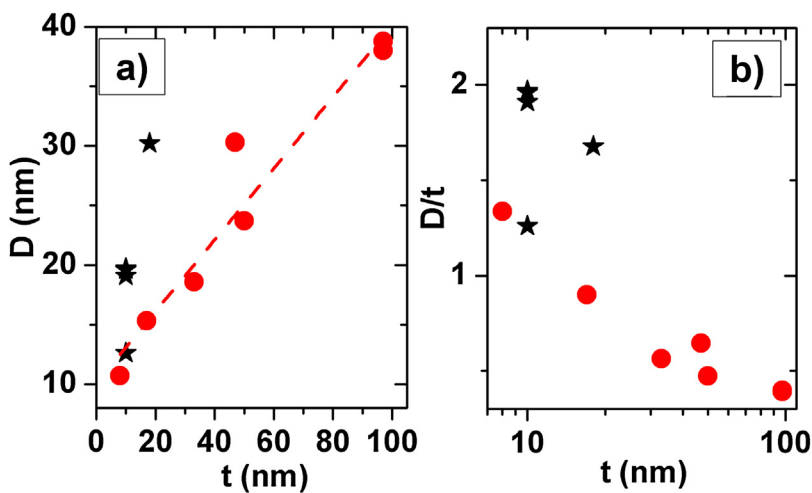


**Fig. 2.** (a) Thickness dependence of mean grain diameter for Au/Cr/Mica (black stars) and Au/Mica samples (red circles). Dashed line represents the best linear adjustment for Au/Mica data. (b) Thickness dependence of the ratio  $D/t$  diameter for Au/Cr/Mica (black stars) and Au/Mica samples (red circles). (For interpretation of the references to colour in this figure legend, the reader is referred to the web version of this article.)

**Table 1**

Morphological and electrical characterizations of Au/Cr/mica and Au/mica samples:  
 $t$ : thickness,  $T_S$ : substrate temperature,  $D$ : mean grain diameter,  $\rho$  (RT): resistivity at room temperature,  $\sigma$ : surface roughness amplitude,  $\Delta\rho/\rho$ : resistivity increase due to thiols adsorption after 25 min.

	$t$ (nm)	$T_S$ (K)	$D$ (nm)	$D/t$	$\rho$ (RT) (nΩm)	$\sigma$ (nm)	$\Delta\rho/\rho$ %
Au/Cr/Mica	10	320	12.6	1.3	57.7	2.2	3.0
	10	350	19.7	2.0	89.1	1.7	7.5
	10	360	19.6	2.0	47.5	1.6	12
	10	390	19.1	1.9	91.4	2.6	0.9
	18	540	30.2	1.7	78.1	5.2	0.3
Au/Mica	8	300	10.7	1.3	110		
	17	300	15.3	0.90	80.2		
	33	300	18.6	0.56	71.6		
	47	300	30.3	0.64	41.4		
	50	300	23.7	0.47	39.4		
	97	300	38.0	0.39	30.8		
	97	300	38.8	0.40	33.7		

the substrate temperature rises, while the resistivity remains low. In order to compare mean grain diameters of different samples we computed the ratio  $D/t$ . Table 1, displays this ratio for all samples. Fig. 2b shows the value of  $D/t$  for all films as a function of thickness. A substrate temperature of about 50 K above RT induces the formation of grains with diameters roughly twice the film thickness. For these substrate temperatures, the electron mean free path  $\lambda_0$  is similar to  $2D$  and  $4t$ , so on average a conduction electron will collide more frequently with the surface than the grain boundaries, thus making the electron-surface scattering the dominant contribution to the resistivity.

It is known that thiol adsorption on a gold film is a surface process that generates new scattering centers affecting the electronic conduction. The resistivity increase due to this effect has been modeled as a reduction of the specularity parameter  $P$  of the upper surface [9,11,12]. Therefore, the magnitude of this resistivity change is directly related to the contribution of the electron-surface scattering to the electrical transport process. Based on this behavior, we used thiol adsorption as a method to distinguish this contribution in Au/Cr/Mica samples.

The fractional resistivity change ( $\Delta\rho/\rho$ ) δυε το τηλισ προχεσσ, is calculated as:

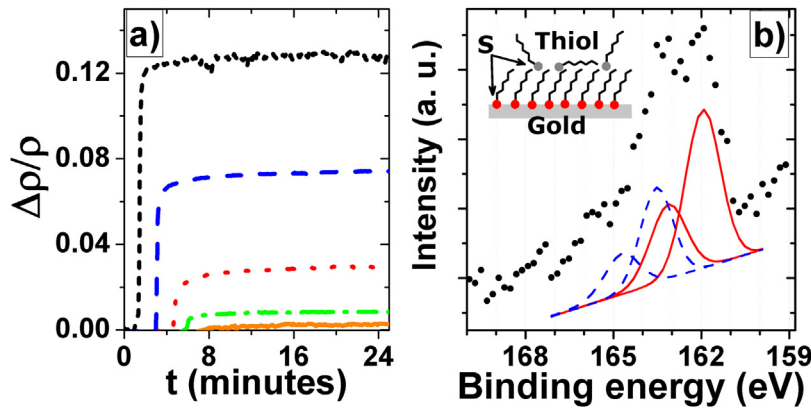
$$\frac{\Delta\rho}{\rho} = \frac{\rho_{\text{with thiols}} - \rho_{\text{without thiols}}}{\rho_{\text{without thiols}}}$$

Fig. 3a shows the time dependence of resistivity increase during dodecanethiol ( $C_{12}$ ) adsorption on Au/Cr/Mica samples. Table 1 shows the values of  $\Delta\rho/\rho$  determined after 25 min of immersion into the  $C_{12}$  solution. The fractional resistivity increments determined here are consistent with other measurements on similar gold films at room temperature. For example, Pugmire et al. [13] showed that  $C_{10}$  adsorption on a 25 nm thick film increases resistivity in 7%. Zhang et al. [9] and Fried et al. [11] reported increments between 2 and 4% after  $C_{16}$  adsorption on 50 nm thick films; and Correa-Puerta et al. [12] observed increments between 0.2 and 2.7% for  $C_{12}$  adsorption on samples with film thickness varying between 28 and 56 nm.

In order to assess the extent of the thiol adsorption, the samples were characterized by XPS after the end of the process. Fig. 4b, shows a typical XPS spectrum from our samples produced by the S-Au bond in the S(2p) region. The S 2p peak is a doublet of  $2p_{3/2}$  and  $2p_{1/2}$  due to spin-orbital splitting, separated by 1.18 eV [25]. Lower continuous lines indicate the doublet observed at 161.9 eV (FMHW = 1.3 eV) corresponding to the S-Au bond. This doublet is interpreted in the literature as molecules bonded to the gold film as a self-assembled monolayer in standing up configuration [26]. The insert in Fig. 3b shows a diagram of the molecules on top of the gold surface. In this configuration we expect the surface to be modified by the bounded molecules, thus, film resistivity is only affected by the presence of the SAM and not by the second unbounded layer. The second doublet (dashed lines), at 163.5 (FMHW = 1.4 eV), corresponds to unbounded sulfur [27]. On the other hand, chromium peaks were not observed, showing that the gold ultrathin film completely covered the chromium layer.

The largest resistivity increases due to thiol adsorption were observed in Au/Cr/Mica films fabricated between 350 and 360 K. It is interesting to contrast this phenomenon with the low resistivity increase (<1%) of films grown at a slightly higher substrate temperature ( $T_S = 390$  K) with similar characteristic dimensions  $\lambda_0 \sim 2D \sim 4t$ . In order to understand this result, we observed their respective morphologies and found that they only differ in the surface roughness amplitude,  $\sigma$ . Fig. 4 shows the resistivity increase, surface roughness and mean grain diameter as a function of substrate temperature.

Fig. 5 shows a representation of the topography of samples fabricated at 390 K and 360 K. The films with the largest resistivity increases after thiol adsorption have small value of  $\sigma$  (right side in Fig. 5), hence a small influence of the initial electron-surface rough-



**Fig. 3.** (a) Time dependence of resistivity increases for different samples. Black short dashed line:  $T_s = 360\text{ K}$ ; Blue dashed line:  $T_s = 350\text{ K}$ ; Red dotted line:  $T_s = 320\text{ K}$ ; Green dash-dotted line:  $T_s = 390\text{ K}$ ; and orange continuous line:  $T_s = 540\text{ K}$ . Starting time of each measurement was displaced 1.5 min for a good presentation of the data. (b) Typical XPS spectrum in S(2p) region. Points correspond to observed spectrum. Lower continuous and dashed lines correspond to resolved peaks. Inset: Diagram of the molecules on top of the gold surface. (For interpretation of the references to colour in this figure legend, the reader is referred to the web version of this article.)

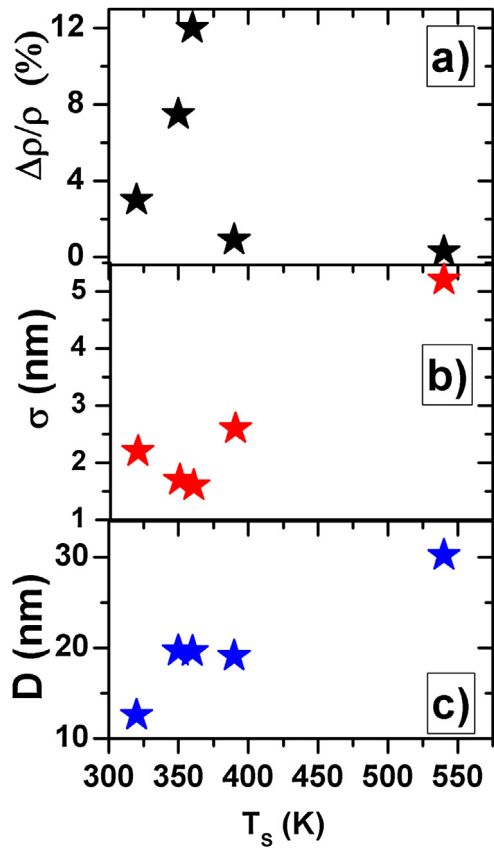


**Fig. 4.** Substrate temperature dependence (a) of resistivity increase due to thiol adsorption, (b) of surface roughness, and (c) of mean grain diameter for Au/Cr/Mica samples.

ness scattering. The films scarcely changing its resistivity after the same treatment are characterized by a larger surface roughness ( $\sigma = 2.6\text{ nm}$ ; left side in Fig. 5) and, conceivably, have the effect of the electron-surface scattering completely saturated from the start.

To validate an experimental procedure, such as the present method of investigating the influence of surface scattering by examining the effect of thiols adsorption on the electrical conductivity; it is necessary to keep in mind that the value of this conductivity is influenced by a number of factors. The majority of these elements are unknown and beyond the control of the experimentalist. Cautionary evidence of this fact resides, for instance, in

our resistivity data in Table 1, where no evident order is discernible. Large variations in the resistivity values presented in similar thin samples were reported by Fenn et al. [28] in 1998. In this work, they fabricated pair of samples with thicknesses ranging from around 5–1000 nm. The evaporated materials were copper and niobium. They observed that, for thicknesses smaller than around 40 nm, the resistivity showed differences between members of each pair, ranging from 20 and 50%. Furthermore, when mica was used as substrate in the case of ultrathin films, these differences were even larger. This is because mica presents some soft cleavage steps that are difficult to detect before the deposition process and, in samples that are too thin, generate a significant resistance enhancement. In these cases the increments in resistivity where not imputable to the scattering mechanisms discussed in this work; and contributed only to obscure the true nature of the mechanisms that control electrical transport.

The use of the present method of thiol adsorption in order to clarify the contribution of the electron-surface scattering presents some advantages over others. First, the method is very sensitive to the possibility of manipulating the strength of this contribution. Further, the alternative method, based on Hall mobility measurements, requires (in the case of noble metals) samples with long mean free paths (that is, of low temperatures) and intense magnetic fields [8]. For example, in the case of the measurements reported in Reference 8, the Hall mobility was measured at 4 K and using magnetic fields up to 4.5 T. Clearly, these conditions are harder to obtain in comparison to the immersion of a sample into a thiol solution. Other approach is the deposition of a second metallic layer. This method, used by Lucas [6], presents two problems. First, since the second layer also conducts electricity, then, the system is transformed into a bilayer with different resistivities depending of composition or fabrication conditions. Second, during the growth of the second layer, as reported by Volmer-Weber [23], gold atoms do not necessarily land on the surface of the film, but instead, on top of atoms of the second layer that had previously arrived. With the method of thiol adsorption, these problems are overcome, S-head of thiols are orderly placed on the gold surface and, since the layer is not a conductor, then thiol overlayer only affects the resistivity of the film by inducing additional scattering centers.

## 5. Conclusions

In order to study the effect of electron-surface scattering in ultrathin films, we prepared gold ultrathin films on mica on top of a chromium seed layer. This layer allows us surpass the electric

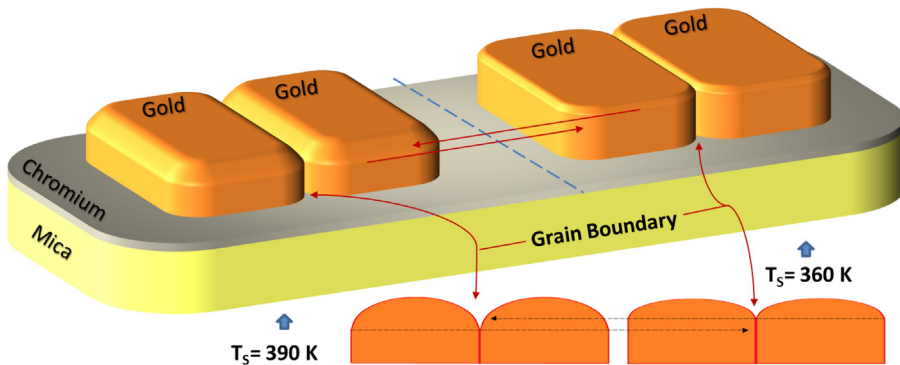


**Fig. 5.** Representation of mean grain diameter and surface roughness for samples fabricated at 390 K and 360 K.

percolation threshold at substrate temperature higher than room temperature. Through the change of substrate temperature during gold deposition, we were able to prepare samples with the same thickness but different topographies. This resulted in samples with varying resistivities, caused by a combination in which the electron scattering mechanisms operate in different proportions. Also, we fabricated gold thin film grown directly on mica, having different thickness, and analyzed the data using Mayadas and Shatzkes theory. We found that in samples with thicknesses lower than 15 nm, electron-surface scattering is the dominant mechanism influencing the film resistivity. Next, we compared the resistivities between both kinds of samples, and found that de discrepancies were caused by observable differences in film morphology between the Au/Cr/Mica and the Au/Mica samples.

To have further evidence on the preponderancy of the surface scattering in comparison to the other scattering mechanisms, we developed the *method of thiol adsorption*. The method consists in comparison of the resistivities before and after the deposition of an ordered, self-assembled monolayer. The film with the highest increase in resistivity is the sample in which electron-surface scattering is predominant. Using this method, we observed that the greater enhancement of electron-surface scattering occurs in samples composed of gold grains with large diameters and small surface roughness amplitudes.

## Acknowledgements

This work was partially financed by project “Fondecyt de Iniciación n° 11140787”. J. C-P. acknowledges “MECESUP grant no. FSM1204” and “PhD Scolarship CONICYT63100001”. C.G-F. acknowledges “PhD Scolarship CONICYT21110732”. L.M. acknowledges support from “Incentivos a la Investigación” of the Universidad Central de Chile. M.F. acknowledges support from “Fondecyt n° 1140759”.

## References

- [1] [www.itrs2.net](http://www.itrs2.net).
- [2] Thorwald Andersson, The electrical properties of ultrathin gold films during and after their growth on glass, *J. Phys. D: Appl. Phys.* 9 (1976) 973.
- [3] R. Henriquez, M. Flores, L. Moraga, G. Kremer, C. González-Fuentes, R.C. Muñoz, Electron scattering at surfaces and grain boundaries in thin Au films, *Appl. Surf. Sci.* 273 (2013) 315–323.
- [4] J.S. Chawla, F. Gstrein, K.P. O'Brien, J.S. Clarke, D. Gall, Electron scattering at surfaces and grain boundaries in Cu thin films and wires, *Phys. Rev. B* 84 (2011) 235423.
- [5] J.M. Rickman, K. Barmak, Simulation of electrical conduction in thin polycrystalline metallic films: impact of microstructure, *J. Appl. Phys.* 114 (2013) 133703.
- [6] M.S.P. Lucas, Surface scattering of conduction electrons in gold films, *Appl. Phys. Lett.* 4 (1964) 73.
- [7] H. Marom, M. Eizenberg, The effect of surface roughness on the resistivity increase in nanometric dimensions, *J. Appl. Phys.* 99 (2006) 123705.
- [8] Ricardo Henriquez, Luis Moraga, German Kremer, Marcos Flores, Andres Espinosa, C. Raul Munoz, Size effects in thin gold films: discrimination between electron-surface and electron-grain boundary scattering by measuring the Hall effect at 4 K, *Appl. Phys. Lett.* 102 (2013) 051608.
- [9] Y. Zhang, R.H. Terrill, P.W. Bohn, Chemisorption and chemical reaction effects on theresistivity of ultrathin gold films at the liquid-solid interface, *Anal. Chem.* 71 (1999) 119.
- [10] Peter Maksymowycz, Oleksandr Voznyy, Daniel B. Dougherty, Dan C. Sorescu, T. John Yates Jr., Gold adatom as a key structural component in self-assembled monolayers of organosulfur molecules on Au(111), *Prog. Surf. Sci.* 85 (2010) 206.
- [11] G.A. Fried, Y. Zhang, P.W. Bohn, Effect of molecular adsorption at the liquid-metal interface on electronic conductivity: the role of surface morphology, *Thin Solid Films* 401 (2001) 171.
- [12] Jonathan Correa-Puerta, Valeria Del Campo, Ricardo Henríquez, Patricio Häberle, Resistivity of thiol-modified gold thin films, *Thin Solid Films* 570 (2014) 150–154.
- [13] D.L. Pugmire, M.J. Tarlov, R.D. Van Zee, Structure of 1,4-benzenedithiol selfassembledmonolayers on gold grown by solution and vapor techniques, *Langmuir* 19 (2003) 3720.
- [14] A.F. Mayadas, M. Shatzkes, Electrical resistivity model for polycrystalline films: the case of arbitrary reflection at external surface, *Phys. Rev. B* 1 (1970) 1382.
- [15] K. Fuchs, The conductivity of thin metallic films according to the electron theory of metals, *Math. Proc. Camb.* 34 (1938) 100.
- [16] E.H. Sondheimer, The influence of a transverse magnetic field on the conductivity of thin metallic films, *Phys. Rev.* 80 (1950) 401.
- [17] M.S.P. Lucas, Electrical conductivity of thin metallic films with unlike surfaces, *J. Appl. Phys.* 36 (1965) 1632.
- [18] R.A. Matula, Electrical resistivity of copper, gold, palladium and silver, *J. Phys. Chem. Ref. Data* 8 (1979) 1147.
- [19] Tik Sun, Bo Yao, Andrew P. Warren, Katayun Barmak, Michael F. Toney, Robert E. Peale, Kevin R. Coffey, Dominant role of grain boundary scattering in the resistivity of nanometric Cu films, *Phys. Rev. B* 79 (2009) 041402.
- [20] Sebastián Bahamondes, Sebastián Donoso, Antonio Ibañez-Landeta, Marcos Flores, Ricardo Henriquez, Resistivity and Hall voltage in gold thin films deposited on mica at room temperature, *Appl. Surf. Sci.* 332 (2015) 694–698.
- [21] J.E. Siewenie, L. He, Characterization of thin metal films processed at different temperatures, *J. Vac. Sci. Technol. A* 17 (1999) 1799.
- [22] Ondřej Kvítek, Peter Konrád, Vaclav Švorčík, Time dependence and mechanism of Au nanostructure transformation during annealing, *Funct. Mater. Lett.* 7 (2014) 1450022.
- [23] S. Bahamondes, S. Donoso, R. Henríquez, M. Flores, Morphological and electrical study of gold ultrathin films on mica, *Thin Solid Films* 548 (2013) 646–649.
- [24] G. Kastle, H.-G. Boyen, B. Koslowski, A. Plettl, F. Weigl, P. Ziemann, Growth of thin flat, epitaxial (111) oriented gold films on c-cut sapphire, *Surf. Sci.* 498 (2002) 168–174.
- [25] D.G. Castner, K. Hinds, D.W. Grainger, X-ray photoelectron spectroscopy sulfur 2p study of organic thiol and disulfide binding interactions with gold surfaces, *Langmuir* 12 (1996) 5083–5086.
- [26] Juanjuan Jia, Angelo Giglia, Marcos Flores, Oscar Grizzi, Luca Pasquali, Vladimir A. Esaulov, 1,4-Benzenedithiol interaction with Au(110), Ag(111), cu(100), and Cu(111) surfaces: self-assembly and dissociation processes, *J. Phys. Chem. C* 118 (2014) 26866–26876.
- [27] Abdulla Hel Al Mamun, Jae Ryang Hahn, Effects of solvent on the formation of octanethiol self-assembled monolayers on Au(111) at high temperatures in a closed vessel: a scanning tunneling microscopy and X-ray photoelectron spectroscopy study, *J. Phys. Chem. C* 116 (2012) 22441–22448.
- [28] M. Fenn, G. Akueyti, P.E. Donovan, Electrical resistivity of Cu and Nb thin films, *J. Phys.: Condens. Matter* 10 (1998) 1707–1720.